Concept of spinning magnetic field at magic-angle condition for line narrowing in Mössbauer spectroscopy

Petr Anisimov* and Yuri Rostovtsev
Department of Physics and Institute for Quantum Studies, Texas A&M University, College Station, Texas 77843-4242, USA

Olga Kocharovskaya
Department of Physics and Institute for Quantum Studies, Texas A&M University, College Station, Texas 77843-4242, USA and Institute of Applied Physics, RAS, Nizhniy Novgorod 603120, Russia

(Received 4 October 2006; revised manuscript received 8 June 2007; published 28 September 2007)

A different technique for narrowing of Mössbauer resonances in crystals is suggested. Similar to high-resolution nuclear magnetic resonance spectroscopy, it uses a combined action of a continuous wave radio-frequency field and a dc magnetic field under a "magic-angle" condition. However, the condition itself is essentially different from the one known previously. Moreover, this technique suppresses the contribution of the dipole-dipole interaction to the energy of Mössbauer transition only (it does not suppress the contribution of the dipole-dipole interaction to the energy of individual levels). It works rather well even in the case of relatively strong dipole-dipole interaction.

DOI: 10.1103/PhysRevB.76.094422 PACS number(s): 76.80.+y

I. INTRODUCTION

Since the experimental discovery of the Mössbauer effect (a physical phenomenon of resonant recoil-free emission and absorption of γ-ray photons by nuclei bound in a crystal) in 1957, it has been observed for nearly 100 nuclear transitions in about 80 nuclides distributed over almost half of all chemical elements. This effect forms the basis of Mössbauer spectroscopy (MS) which has a number of applications, especially in solid state physics and chemistry.[1–5]

Fundamentally, the width of recoilless γ-ray resonances, Mössbauer resonances, is limited only by the radiative linewidth of the given nuclear transition. However, inhomogeneous broadening, $\delta\omega_{inh}$, often sets a limit on the width of Mössbauer resonances. In particular, for transitions with a lifetime longer than 10 μs, $\delta\omega_{inh}$ defines the ultimate width of Mössbauer resonances. Large inhomogeneous broadening of long-lived recoilless transitions, as compared to the radiative broadening, is the major factor restricting their applications in Mössbauer spectroscopy. (Homogeneous broadening caused by spin-lattice relaxation can be suppressed down to 0.1 Hz by cooling a sample below 1 K.) In the case of nuclear transitions with a lifetime shorter than 10 μs, $\delta\omega_{inh}$ may sometimes exceed the radiative linewidth and limit the resolution of MS. An example of such a transition is the 14.4 keV transition in ^{57}Fe. For this transition, the width of Mössbauer resonances in some compounds may be four to nine times larger than the radiative linewidth.[6,7] Therefore, the suppression of inhomogeneous broadening would both improve the resolution of Mössbauer spectroscopy in the cases where an interaction with an environment prevents an accurate measurement and allow for extension of the Mössbauer technique to the longer-lived isomers and for observing Mössbauer resonances narrower than those currently achieved.

Inhomogeneous broadening also sets a fundamental obstacle to the realization of a Mössbauer γ-ray laser. The original idea of the Mössbauer γ-ray laser was suggested in 1961 by Rivlin.[8] For lasing to occur, the net gain should exceed off-resonance losses caused by ionization and Compton scattering of γ radiation in crystals. The net resonant gain, in turn, is proportional to the ratio of the radiative linewidth to the total linewidth. For sufficiently long-lived isomers (for which pumping could be feasible), this ratio is very small. Thus, an increase of this ratio via the suppression of inhomogeneous broadening would lead to a dramatic release in the amplification condition, as discussed in the literature devoted to the problem of γ-ray laser.[9,10]

The inhomogeneous broadening of Mössbauer resonances is caused by the inhomogeneities of hyperfine (HF) interactions. This mechanism is essentially the same as in the case of nuclear magnetic transitions in solids. Very efficient methods of suppression of inhomogeneous broadening down to 0.1 Hz have been developed in high-resolution solid state nuclear magnetic resonance spectroscopy (HRSSNMRS).[11] The field of HRSSNMR started with the pioneering work of Andrew *et al.*[12,13] They showed that mechanical spinning of a sample can greatly reduce the width of nuclear magnetic resonances if the axis of rotation makes a particular angle with a constant magnetic field. The same result was achieved by the application of a radio-frequency (rf) field without rotation of the sample.[11] Finally, apart from the mechanical spinning of a sample, two different techniques have been developed. The first one uses sequences of resonant $\pi/2$ rf pulses.[14,15] The second one exploits a slightly detuned continuous rf field satisfying a "magic-angle" condition.[16] Both techniques are based on the symmetry of the HF interactions which allows the suppression of the contribution of the HF interactions down to zero if such a contribution is sufficiently small.

For the last 40 years, HRSSNMRS has been developed into the flourishing field of research and applications. Therefore, the extension of the techniques of HRSSNMRS to Mössbauer spectroscopy appears to be promising. The mechanical rotation of a sample would be inappropriate since MS essentially uses the Doppler effect for changing the transition frequency. However, the application of a rotating rf field is possible. The influence of the rf field on the Mössbauer resonance was widely studied theoretically since the

1960s;[17] see also Refs. 18–22 for reviews. Some coherent effects in MS caused by the rf field, such as collapse of the HF structure,[23–25] ac-Stark splitting,[26–29] and two-photon gamma-rf transitions,[30–32] were observed experimentally. The idea to apply the HRSSNMRS techniques to narrow Mössbauer resonances was pioneered in the 1970s. It was suggested to use sequences of $\pi/2$ rf pulses[33] or quasicontinuous rf fields.[9] The peculiarity of MS as compared to HRSSNMRS lies in the presence of HF structure in an excited nuclear state as well as in a ground nuclear state. For example, the dipole-dipole interaction couples pairs of nuclei in a ground state as well as in an excited state; moreover, it couples pairs of nuclei one of which is in a ground and the other one is in an excited state. Thus, the idea presented in the previous papers[9,33] was to suppress HF interactions both in ground and excited nuclear states. The outcome of such an approach would be simultaneous elimination of all possible contributions from HF interactions. The drawback of such an approach was the requirement for rather complicated sequence of cycles of bichromatic rf field. One rf frequency was meant to affect ground nuclear states, while the other was supposed to affect excited nuclear states only. After all, line narrowing was still limited by the fact that each rf frequency was affecting both ground and excited nuclear states. As far as we know, no experimental attempts for the verification of this proposal were undertaken.

In our recent papers,[34,35] we considered the possibility to narrow Mössbauer resonances by a monochromatic cw rf field. We used a combination of a traditional magic-angle condition with effective time averaging. It was shown that partial narrowing could be achieved and that an optimization of the parameters used is required for further improvement.

In this paper, we suggest an essentially different approach for the suppression of the inhomogeneous broadening of Mössbauer resonances caused by the dipole-dipole interaction. Namely, we look for a condition where the contribution of the dipole-dipole interaction to the frequency of a Mössbauer resonance vanishes under the action of a monochromatic continuous rf field. At the same time, we are not attempting full suppression of the dipole-dipole interaction and its contributions to the energy of individual levels. The frequency of γ-ray absorption remains well defined even though the energy of individual nuclear levels deviates significantly. This happens due to the cancellation of these deviations when the energy difference is observed. In this way, we define the magic-angle condition for MS and show that efficient suppression of the inhomogeneous broadening of Mössbauer resonances becomes possible with one monochromatic continuous rf field.

II. THEORETICAL MODEL

A typical Mössbauer experiment involves a nuclear transition between two levels, with energy separation of about 10–100 keV. Each nuclear level has sublevels with a definite projection of the nuclear moment onto a quantization axis. The energy separation of nuclear sublevels is on the order of 10 neV. These sublevels are actually responsible for the HF structure of observed spectra. In a typical Mössbauer setup,

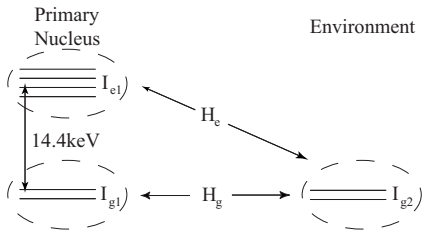

FIG. 1. Schematic representation of the studied system in the case of ^{57}Fe. H_g and H_e represent an interaction of the primary nucleus in the ground and excited states with its environment, respectively.

the flux of incident γ photons from a radioactive source is not sufficient to excite several nuclei in the close vicinity of each other. Therefore, one can always consider that only one (primary) nucleus interacts with γ radiation and the rest of the nuclei (of the same type as the primary nucleus or some different nuclei in the crystal host) represent the environment and cannot be excited. For the sake of further discussion, we label the primary nucleus as "1" and a nucleus from the environment as "2" (see Fig. 1).

In order to introduce the inhomogeneous broadening in our system, we assume that the primary nucleus interacts with the environment through the dipole-dipole interaction. This is a short-range pairwise interaction, which depends on a distance r_0 between the nuclei in the pair and on a relative position $\mathbf{n}_0=(\cos\phi\sin\theta,\sin\phi\sin\theta,\cos\theta)$ of the pair with respect to the axis of quantization (z axis). Short-range interactions mostly involve the nearest nuclei. Therefore, we assume r_0 to be constant and equal to the distance between nuclei. Furthermore, due to the pairwise nature of the dipole-dipole interaction, we can reduce our system to the pair of nuclei, which contains the primary nucleus and a nucleus from the environment. Thus, in order to calculate a bulk response, one has to average the pairwise response over θ and ϕ.

Our system has a close resemblance to the one used to describe HRSSNMR except for the possibility of the primary nucleus to be in the excited state. Thus, there are two contributions to the width of Mössbauer resonances instead of one contribution to the width of nuclear magnetic resonances. The first contribution is due to the interaction of the primary nucleus in the ground state with the environment, H_g, and is also present in the case of HRSSNMR. The second contribution comes from the interaction of the primary nucleus in the excited state with the environment, H_e, and is specific for Mössbauer resonances. Thus, the HRSSNMR techniques have to be modified to consider this contribution.

For all further estimates and numerical simulations, we assume the primary nucleus to be ^{57}Fe in a soft ferromagnetic material.[36] Such nuclei experience a strong internal magnetization, which can be easily manipulated in soft ferromagnets by a rather weak external magnetic field. In principle, the environment may contain nuclei other than ^{57}Fe. However, for further estimates, we also use all typical characteristics of ^{57}Fe except for the magnitude of the dipole-dipole coupling constant. At the atomic distances, the dipole-dipole interaction between ^{57}Fe is relatively weak when

compared to the width of the Mössbauer resonance. For the sake of demonstration, we assume that the dipole-dipole coupling constant $\eta \sim \frac{\mu_1 \mu_2}{r_0^3}$ (where μ_i is the magnetic dipole moment of the ith nucleus) is large enough to provide substantial inhomogeneous broadening of the Mössbauer spectrum.

In order to achieve the suppression of inhomogeneous broadening, we place the system in the external magnetic field which consists of two components: a constant component (this component defines the z axis) and a time-dependent one. We choose the time-dependent component in such a way that the total external magnetic field spins around the z axis: $\mathbf{B}=B_0(r\cos\omega_{rf}t, -r\sin\omega_{rf}t, 1)$. In the previous expression, we introduced r as the ratio of the magnitudes of the time-dependent and the constant components of the magnetic field.

The Hamiltonian of the system consisting of the pair of nuclei placed in the external magnetic field and coupled through the dipole-dipole interaction is written as follows ($\hbar=1$):

$$H = -\mathbf{B}(\gamma_1\mathbf{I}_1 + \gamma_2\mathbf{I}_2) + \eta[\mathbf{I}_1\mathbf{I}_2 - 3(\mathbf{n}_0\mathbf{I}_1)(\mathbf{n}_0\mathbf{I}_2)], \quad (1)$$

where γ_i and $\mathbf{I}_i$ are the gyromagnetic ratio and the nuclear moment of the **i**th nucleus. For our system, γ_1 and $\mathbf{I}_1$ are not fixed and depend on the state of the nucleus; however, γ_2 and $\mathbf{I}_2$ are fixed to $\gamma_g = 1.373\ \mathrm{MHz\,T^{-1}}$ and $\mathbf{I}_g = \frac{1}{2}$, respectively, since the second nucleus can be in the ground state only. For the primary nucleus, the gyromagnetic ratio and the nuclear moment can also be equal to $\gamma_e = -0.787\ \mathrm{MHz\,T^{-1}}$ and $\mathbf{I}_e = \frac{3}{2}$ if the nucleus is in the excited state.

Depending on the state of the primary nucleus, the system can be in the ground state described by the Hamiltonian

$$H_g = -\mathbf{B}(\gamma_g\mathbf{I}_{g1} + \gamma_g\mathbf{I}_{g2}) + \eta_g[\mathbf{I}_{g1}\mathbf{I}_{g2} - 3(\mathbf{n}_0\mathbf{I}_{g1})(\mathbf{n}_0\mathbf{I}_{g2})] \quad (2)$$

or in the excited state, with energy $\hbar\Omega_0 = 14.4$ keV, described by the Hamiltonian

$$H_e = -\mathbf{B}(\gamma_e\mathbf{I}_{e1} + \gamma_g\mathbf{I}_{g2}) + \eta_e[\mathbf{I}_{e1}\mathbf{I}_{g2} - 3(\mathbf{n}_0\mathbf{I}_{e1})(\mathbf{n}_0\mathbf{I}_{g2})], \quad (3)$$

where $\frac{\eta_e}{\eta_g} = \frac{\gamma_e}{\gamma_g} = -0.573$. The energy of the excited state is omitted here, a condition which is equivalent to the rotating wave approximation in quantum optics.[37]

For H_g, we have two nuclei with $I_{g1} = \frac{1}{2}$ and $I_{g2} = \frac{1}{2}$, which leads to the basis $|\frac{1}{2}, m_1 = \frac{1}{2}, -\frac{1}{2}\rangle \otimes |\frac{1}{2}, m_2 = \frac{1}{2}, -\frac{1}{2}\rangle$. However, as shown in our previous work,[35] the basis of the total moment, $|0,0\rangle$, $|1,1\rangle$, $|1,0\rangle$, and $|1,-1\rangle$, is the most useful for a system of two identical nuclei. This observation is based on the fact that a state with a total moment equal to zero $|0,0\rangle$ is not affected by magnetic interactions. Thus, it can be excluded from consideration.

For H_e, the primary nucleus has $I_{e1} = \frac{3}{2}$, which leads to the basis $|\frac{3}{2}, m_1 = \frac{3}{2}, \ldots, -\frac{3}{2}\rangle \otimes |\frac{1}{2}, m_2 = \frac{1}{2}, -\frac{1}{2}\rangle$. In this case, there is no actual preference for the basis of the total moment.

The Mössbauer transition in the primary nucleus from the ground to the excited level is considered to be magnetic dipole allowed (corresponding to the case of ^{57}Fe). It means that a transition operator can be written as $V = -\hat{\mu}\cdot\mathbf{B}_\gamma$. In the previous expression, we introduced the magnetic field of a γ quantum, $\mathbf{B}_\gamma$, and the magnetic moment of the transition, $\hat{\mu}$. The magnetic moment $\hat{\mu}$ is proportional to $\Sigma_{m=-1}^{1}\hat{\mu}_m\cdot\mathbf{X}_m$, where $(\hat{\mu}_m)_{m_e,m_g} = \langle I_g, 1, -m_g, m || I_e, m_e\rangle$ are the Clebsch-Gordan coefficients[38] and $\mathbf{X}_0 = \mathbf{z}_0$, $\mathbf{X}_{\pm 1} = \mp\frac{1}{\sqrt{2}}(\mathbf{x}_0 \pm i\mathbf{y}_0)$. We assume that an incident γ radiation propagates along the y axis and can have either $\mathbf{B}_\gamma \| \mathbf{z}_0$ or $\mathbf{B}_\gamma \| \mathbf{x}_0$. Hence, the transition operator is represented by the matrix V_z^0 in the case of $\mathbf{B}_\gamma \| \mathbf{z}_0$ or by the matrix V_x^0 in the case of $\mathbf{B}_\gamma \| \mathbf{x}_0$:

$$V_z^0 = K\begin{bmatrix} 0 & 0 \\ \sqrt{2} & 0 \\ 0 & \sqrt{2} \\ 0 & 0 \end{bmatrix}, \quad V_x^0 = \frac{K}{\sqrt{2}}\begin{bmatrix} -\sqrt{3} & 0 \\ 0 & -1 \\ 1 & 0 \\ 0 & \sqrt{3} \end{bmatrix}, \quad (4)$$

where K is some constant which is irrelevant for further discussion. Here, the following basis for the primary nucleus is assumed: $|I_e = \frac{3}{2}, m_e = \frac{3}{2}, \ldots, -\frac{3}{2}\rangle$ for the excited and $|I_g = \frac{1}{2}, m_g = \frac{1}{2}, -\frac{1}{2}\rangle$ for the ground state. Finally, the transition matrices for our system of two nuclei with one nucleus confined to the ground state are $\tilde{V}_{x,z}^0 = V_{x,z}^0 \otimes \hat{1}_{2\times 2}$, which have to be transformed to the basis discussed above.

We calculate Mössbauer spectra based on the Floquet-state perturbation theory presented in Refs. 34 and 39. This theory was developed to study homogeneously broadened Mössbauer spectra under the influence of the rf field. It treats γ radiation as a perturbation which is always the case for MS allowing for a nonperturbative treatment of the rf field. It is important to note that it also allows for a nonperturbative analysis of the dipole-dipole interaction. As far as we know, nobody has used this method to study inhomogeneously broadened Mössbauer spectra (the broadening caused by the dipole-dipole interaction). This theory predicts a time-averaged absorption spectrum to be the sum of the Lorentzians:

$$L = |V_k(e,g)|^2 \frac{2}{\pi}\frac{\Gamma}{(\Omega - \Omega_{n,m,k})^2 + \Gamma^2}, \quad (5)$$

where $V_k(e,g) = \frac{1}{T}\int_0^T \langle n_e|\tilde{V}_{x,z}^0|m_g\rangle e^{ik\omega_{rf}t}dt$ is the kth coefficient of the Fourier series of the matrix element of the transition operator $\tilde{V}_{x,z}^0$ between the Floquet states $|n_e\rangle$ and $|m_g\rangle$; $\Omega_{n,m,k} = \Omega_0 + E_{\{n\}}^e - E_{\{m\}}^g - k\omega_{rf}$ is the resonance frequency of the corresponding transition.

III. GROUND STATE MAGIC-ANGLE CONDITION

The strength of the dipole-dipole interaction can be judged by $\frac{\eta_g}{|\Delta_{eff}|}$, the ratio of the coupling constant to the Zeeman splitting in the effective magnetic field, which is defined in Appendix A. If the ratio is small, then the dipole-dipole interaction can be treated by perturbation method. First, we consider the primary nucleus in the ground state and the ratio being small. In this case, our system is described in the corotating frame of reference by a so-called truncated Hamiltonian (see Ref. 40):

$$H_g^0 = -\gamma_g(\mathbf{B}_{eff})_g(\mathbf{I}_{g1}+\mathbf{I}_{g2}) - \eta_g A[\mathbf{I}_{g1}\cdot\mathbf{I}_{g2} - 3(\mathbf{I}_{g1})_z(\mathbf{I}_{g2})_z], \tag{6}$$

where I_{gi} is the nuclear moment of the ith nucleus, γ_g is the gyromagnetic ratio, η_g is the dipole-dipole coupling for the ground state, and $A=3\cos^2\theta-1$ represents the dependence of the interaction Hamiltonian on the relative position of the nuclear pair. Eigenvalues of H_g^0 in the absence of the dipole-dipole interaction are $\{0,\Delta_{eff},0,-\Delta_{eff}\}$ (see Appendix A), which are the dynamical energy levels corresponding to the states dressed by the rf field with a corresponding total moment equal to 0 for the first eigenvalue and 1 for the last three eigenvalues. The dipole-dipole interaction provides an additional contribution to the eigenvalues:

$$\{0,-\eta_g D(\theta_{eff}),2\eta_g D(\theta_{eff}),-\eta_g D(\theta_{eff})\}. \tag{7}$$

These linear corrections are proportional to $D(\theta_{eff})=\frac{A}{8}(3\cos^2\theta_{eff}-1)$, and thus can be set to zero all at once if

$$3\cos^2\theta_{eff}-1=0. \tag{8}$$

This condition is well known in solid state high-resolution nuclear magnetic resonance spectroscopy as the magic-angle condition, which defines the magic angle as $\theta_{eff}=\arccos\left(\frac{1}{\sqrt{3}}\right)$.

IV. STRONG DIPOLE-DIPOLE INTERACTION IN THE GROUND STATE

A typical value of the magnetic field experienced by ^{57}Fe in the soft ferromagnets is on the order of 30 T. In such a field, a Zeeman splitting is $\frac{|\Delta|}{2\pi}=41.2$ MHz, i.e., it exceeds the radiative linewidth, which is equal to $\frac{2\Gamma}{2\pi}=2.256$ MHz, only by a factor of 18. Thus, if the inhomogeneous broadening caused by the dipole-dipole coupling exceeds the radiative linewidth, then this coupling should be relatively strong, so that the ratio $\frac{\eta_g}{|\Delta|}$ cannot be smaller than 1/18. In other words, a range of the dipole-dipole coupling constants where the magic-angle condition works well is quite narrow: 2.256 MHz $<\frac{\eta_g}{2\pi}\ll 41.2$ MHz.

When the dipole-dipole constant becomes comparable to or even exceeds Zeeman splitting, $\frac{\eta_g}{|\Delta_{eff}|}\geqslant 1$, we cannot use perturbation theory anymore. In this case, the energies of the ground state should be calculated numerically. We are going to use Floquet analysis according to the prescription outlined in Appendix B.

Figure 2 presents quasienergies (circles) of the Floquet states, which correspond to the states with a total nuclear moment equal to 1, in the case $\frac{\eta_g}{2\pi}=9.024$ MHz. There are more than three values at each particular frequency ω_{rf}, but unique points are confined to the first Floquet zone, which lies in between two dashed lines $\pm\frac{\omega_{rf}}{2}$.

In the absence of the dipole-dipole interaction, quasienergies can be calculated analytically. They are represented by the solid lines marked as ε_1, ε_0, and ε_{-1}.

The frequencies of the rf field satisfying the magic-angle condition [defined by Eq. (8) for the chosen parameters] are presented by the vertical short-dashed lines in Fig. 2.

As it is obvious in Fig. 2, the higher value of the frequency satisfying to magic-angle condition (which lies above the nuclear magnetic resonance frequency for the ground state $\frac{\omega_{rf}}{2\pi}=41.2$ MHz) does not correspond to the vanishing contribution of the dipole-dipole interaction to the ground state energy. It is less obvious for the lower value of the frequency. Therefore, we provide a closer look at the selected area in Fig. 3. Moreover, we plot the normalized difference between an exact numerical value of the energy and that obtained analytically in the absence of the dipole-dipole interaction:

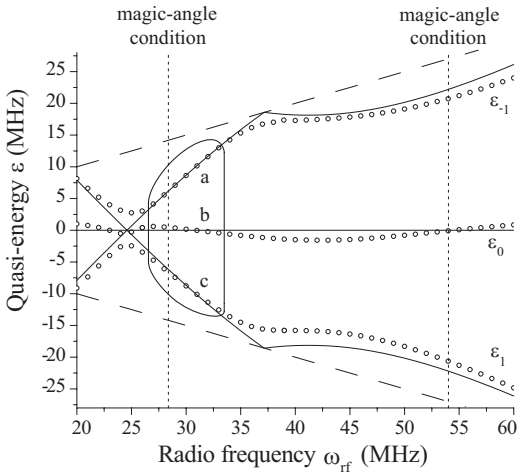

FIG. 2. Quasienergies of H_g as a function of the rf frequency for the states with the total moment equal to 1. These values, marked by circles, are calculated for the following set of parameters: $\frac{\eta_g}{2\pi}=9.024$ MHz, $r=0.44$, $\frac{\Delta}{2\pi}=41.2$ MHz, and $\theta=\frac{\pi}{4}$. Solid lines labeled by ε_1, ε_0, and ε_{-1} correspond to the quasienergies of H_g calculated analytically in the absence of the dipole-dipole interaction. Dashed lines represent the limits of the Floquet zone. Vertical short-dashed lines correspond to the magic-angle condition. More detailed analysis of the selected region is presented in Fig. 3.

$$\frac{\Delta\varepsilon}{\Gamma}=\frac{\varepsilon^{num}-\varepsilon^0}{\Gamma}. \tag{9}$$

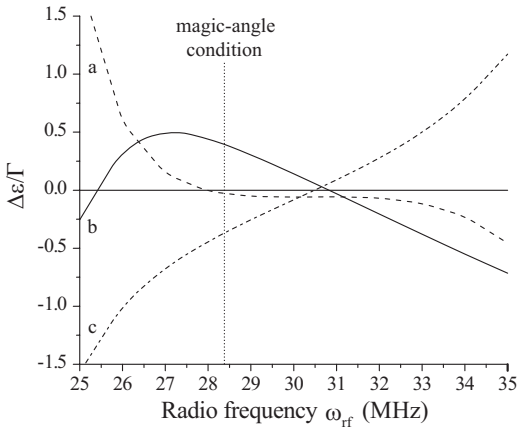

FIG. 3. The normalized difference between the numerical value of the quasienergy of the ground state and the value obtained analytically in the absence of the dipole-dipole interaction [see Eq. (9)] as a function of ω_{rf} is represented. The parameters are the same as in Fig. 2.

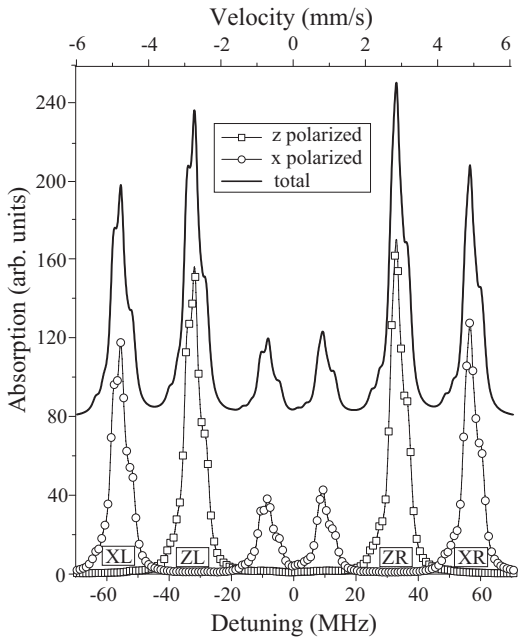

FIG. 4. Mössbauer absorption spectrum calculated in the presence of a constant magnetic field $B_0=30$ T and a strong dipole-dipole interaction in the ground state only: $\frac{\eta_g}{2\pi}=9.024$ MHz and $\frac{\eta_e}{2\pi}=0$ MHz. The dipole-dipole interaction results in a substantial broadening of the Zeeman sextet. The four strongest Mössbauer resonances are labeled accordingly: ZL and ZR for z-polarized radiation and XL and XR for x-polarized radiation. A shift of 80 arbitrary units is introduced to separate the spectrum for unpolarized radiation from its polarized contributions.

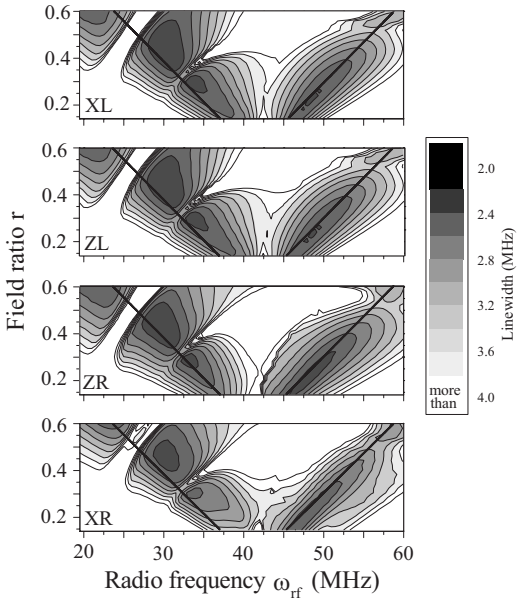

FIG. 5. The dependence of the width of the four major Mössbauer resonances on the frequency ω_{rf} and the relative strength r of the rf field is presented. All parameters are the same as in Fig. 4. A shade coding is used such that the darker shade corresponds to the smaller width of a resonance. In order to provide a better resolution, values greater than 4 MHz are whited out. Along solid lines, ω_{rf} and r satisfy the ground state magic-angle condition defined by Eq. (8).

As it follows from Fig. 3, only ε_{-1} is unaffected by the dipole-dipole coupling at magic-angle condition. The contribution of the dipole-dipole interaction to ε_0 and ε_1 does not vanish at magic-angle condition. Finally, it is important to note that it is possible to minimize the ground state dipole-dipole contribution, if $\omega_{rf}=30.7$ MHz, for all three quasienergies at once.

Let us study how the dipole-dipole coupling in the ground state affects a Mössbauer spectrum. For this purpose, we temporarily put $\eta_e=0$ (see also Ref. 34) and use the same coupling constant $\frac{\eta_g}{2\pi}=9.024$ MHz as above. This coupling is strong enough to provide a noticeable broadening of the Mössbauer resonances (see Fig. 4). This figure contains contributions from x- and z-polarized γ radiation which sums up to a total spectrum for unpolarized radiation. One can see that there are four major Mössbauer resonances: two for x- and two for z-polarized radiation which are marked accordingly as XR, XL, ZR, and ZL in Fig. 4.

We calculated Mössbauer absorption spectra for a broad range of parameters of the rf field. Figure 5 presents dependence of the width of the four strongest Mössbauer resonances on the relative strength r (vertical scale) and the frequency ω_{rf} (horizontal scale) of the rf magnetic field. As it could be expected, the regions where the linewidth reaches its minimal value extend along the solid lines defined by the magic-angle condition [see Eq. (8)]. However, due to the large strength of the dipole-dipole interaction, the actual minima for XR and ZR, which involve ε_1, are shifted to the higher values of ω_{rf}. This result could be expected based on the behavior of ε_1 described in the beginning of this section.

Table I summarizes the analysis of the ground state contribution to the width of Mössbauer resonances and contains numerical values of the ground state contribution to the width of the four major Mössbauer resonances. This contribution was estimated as $\Delta\omega_d=\Delta\omega_{inh}-2\Gamma$, where $\Delta\omega_{inh}$ is the total linewidth and 2Γ is the linewidth in the absence of the dipole-dipole interaction. The first row of Table I presents the dipole-dipole contributions in the absence of the rf field. The next four rows show absolute minima of $\Delta\omega_d$ for each of the four strongest Mössbauer resonances with corresponding labels presented in the last column. The last row of Table I corresponds to the minimum of the function defined as follows:

$$F(r,\omega_{rf})=0.5\sum_{\alpha\&\beta\in\Omega}[(\Delta\omega_d)_\alpha-(\Delta\omega_d)_\beta]^2, \qquad (10)$$

where $\Omega=\{\mathrm{XL},\mathrm{ZL},\mathrm{ZR},\mathrm{XR}\}$ and $(\Delta\omega_d)_\alpha$ is a contribution of the dipole-dipole coupling to the width of the Mössbauer resonance marked by α.

A final conclusion of this section is that suppression of the ground state contribution is possible. However, it does not happen at the magic-angle condition and needs an adjustment of the parameters. Moreover, efficient suppression requires different sets of parameters for each Mössbauer resonance. Nevertheless, Table I shows that a compromise can be found and an equivalent suppression can be achieved simul-

TABLE I. Contribution of the ground state dipole-dipole coupling to the width of the four strongest Mössbauer resonances. The first row presents contributions in the absence of the rf field. The next four rows present residual contributions after applying the rf field. Each row corresponds to maximal suppression for a particular Mössbauer resonance, specified in the last column. The last row presents parameters and values corresponding to the case when function defined in Eq. (10) reaches minimum, which means that all four Mössbauer resonances have residual contributions of the same order.

ω_{rf} (MHz)	r	$\Delta\omega_d$ for XL (MHz)	$\Delta\omega_d$ for ZL (MHz)	$\Delta\omega_d$ for ZR (MHz)	$\Delta\omega_d$ for XR (MHz)	Abs min for
0	0	3.2546	3.3171	3.7089	3.6831	
29.66	0.4614	0.1716	0.1814	0.2054	0.1953	XL
30	0.4517	0.1781	0.1651	0.2012	0.2068	ZL
29.56	0.4398	0.1848	0.1809	0.1857	0.1891	ZR
29.39	0.4472	0.1846	0.1911	0.1921	0.1861	XR
29.989	0.4108	0.19845	0.19863	0.20071	0.20102	Optimal

taneously for all the strongest Mössbauer resonances (see Fig. 6).

V. EXCITED STATE "MAGIC-ANGLE" CONDITION

In this section, we consider the primary nucleus in the excited state. When the contribution of the dipole-dipole interaction to the energy of the excited state is small, $\frac{\eta_e}{|\Delta_{eff}|} \ll 1$ it can be treated perturbatively, similar to the analysis carried out for the ground state in Sec. IV. In a corotating frame of reference, the truncated Hamiltonian for the excited state (taking into account the dipole-dipole coupling in the first order of the perturbation theory) takes the form

$$H_e^0 = -\gamma_e(\mathbf{B}_{eff})_e \cdot \mathbf{I}_{e1} - \gamma_g(\mathbf{B}_{eff})_g \cdot \mathbf{I}_{g2} + \eta_e A[\mathbf{I}_{e1} \cdot \mathbf{I}_{g2} - 3(\mathbf{I}_{e1})_z(\mathbf{I}_{g2})_z], \quad (11)$$

where $(\mathbf{B}_{eff})_g$ and $(\mathbf{B}_{eff})_e$ are the different effective magnetic fields for the magnetic dipole moments in the ground and excited states, respectively, $I_{(g/e)i}$ and $\gamma_{g/e}$ are the nuclear moment of the ith nucleus and the gyromagnetic ratio for the ground and/or excited state, η_e is the dipole-dipole coupling for the excited state, and $A=3\cos^2\theta-1$ represents a dependence on the relative position. Eigenvalues of H_e^0 in the absence of the dipole-dipole interactions are

$$\frac{3}{2}\Delta_{eff}^e \pm \frac{1}{2}\Delta_{eff}^g, \quad (12)$$

$$\frac{1}{2}\Delta_{eff}^e \pm \frac{1}{2}\Delta_{eff}^g, \quad (13)$$

$$-\frac{1}{2}\Delta_{eff}^e \pm \frac{1}{2}\Delta_{eff}^g, \quad (14)$$

$$-\frac{3}{2}\Delta_{eff}^e \pm \frac{1}{2}\Delta_{eff}^g \quad (15)$$

(see Appendix A).

Since there are two different effective fields, the magic-angle condition for only one effective angle becomes meaningless now. Nevertheless, some condition connecting two parameters of the rf field, namely, its relative strength r and its frequency ω_{rf}, can be derived based on the requirement of vanishing of the linear order corrections to the energy of the excited state.

$$\{\mp 3\eta_e\tilde{D}, \mp \eta_e\tilde{D}, \pm \eta_e\tilde{D}, \pm 3\eta_e\tilde{D}\}. \quad (16)$$

These corrections are proportional to the following function of the two arguments:

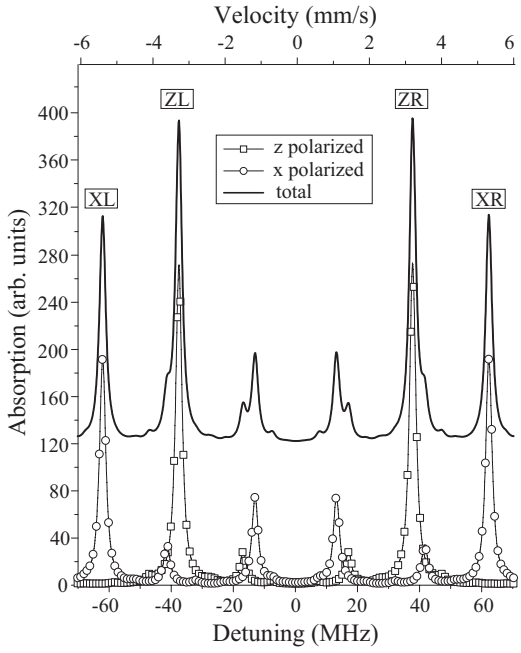

FIG. 6. Mössbauer absorption spectrum calculated in the presence of the spinning magnetic field with the following parameters: $B_0=30$ T, $r=0.4108$, and $\omega_{rf}=29.989$ MHz. The dipole-dipole coupling constants are $\frac{\eta_g}{2\pi}=9.024$ MHz and $\frac{\eta_e}{2\pi}=0$ MHz. A shift of 120 arbitrary units is introduced to separate the spectrum for unpolarized radiation from its polarized contributions. The residual ground state contribution to the width of the strongest Mössbauer resonances is given in Table I.

$$\tilde{D}(\theta^g_{eff}, \theta^e_{eff}) = \frac{A}{8}\left[3\cos^2\left(\frac{\theta^e_{eff}+\theta^g_{eff}}{2}\right) - 1 - \sin^2\left(\frac{\theta^e_{eff}-\theta^g_{eff}}{2}\right)\right], \quad (17)$$

which reduces to $D(\theta_{eff})$ in the case of $\theta^e_{eff}=\theta^g_{eff}$. Zero values of $\tilde{D}(\theta^g_{eff}, \theta^e_{eff})$ define the following condition for the suppression of the linear order correction to the energy of the excited state:

$$3\cos^2\left(\frac{\theta^e_{eff}+\theta^g_{eff}}{2}\right) - 1 - \sin^2\left(\frac{\theta^e_{eff}-\theta^g_{eff}}{2}\right) = 0. \quad (18)$$

VI. STRONG DIPOLE-DIPOLE INTERACTION IN THE EXCITED STATE

When the dipole-dipole coupling constant η_e becomes comparable to or even exceeds Zeeman splitting in the excited state, the dipole-dipole interaction cannot be treated perturbatively. Similar to the case of the ground state, the energies of the excited state can be calculated numerically using the Floquet analysis.

Modification of the Mössbauer absorption spectrum due to the dipole-dipole interaction in the excited state is demonstrated in Fig. 7. Here, we assume that $\frac{\eta_e}{2\pi}=-5.171$ MHz and $\eta_g=0$. According to the relationship $\eta_e=\frac{\gamma_e}{\gamma_g}\eta_g=-0.573\,\eta_g$, the dipole-dipole coupling constant $\frac{\eta_e}{2\pi}=-5.171$ MHz corresponds to the previously used ground state coupling constant $\frac{\eta_g}{2\pi}=9.024$ MHz.

The contribution of the dipole-dipole couplings in the ground and excited states to the widths of the Mössbauer resonances can be seen in Table II. Note that the contribution to the excited state, $\Delta\omega_d$, for x-polarized radiation is larger than for z-polarized radiation. It is due to the fact that the corresponding transitions involve states with three times larger projection of the nuclear moment. Finally, when both contributions are combined, the Zeeman sextet becomes hard to recognize (see Fig. 8) because inhomogeneous broadening becomes comparable to the separation between the Mössbauer resonances (see the last row of Table II).

VII. MAGIC ANGLE CONDITION FOR NARROWING OF THE MÖSSBAUER RESONANCES

In order to suppress the dipole-dipole coupling both in the ground and excited states (when this coupling is relatively week) in the presence of the spinning magnetic field, two

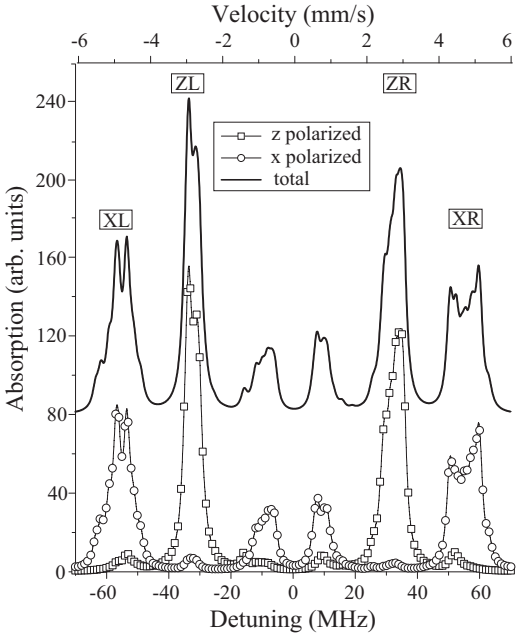

FIG. 7. Broadening of the Mössbauer resonances caused by the dipole-dipole interaction in the excited state assuming that $\frac{\eta_e}{2\pi}=-5.171$ MHz and $\eta_g=0$. The shift of 80 arbitrary units is introduced to separate the spectrum for unpolarized radiation from its polarized contributions.

different magic-angle conditions derived above [Eqs. (8) and (18)] should be fulfilled. However, it is easy to see that it is impossible to satisfy both conditions simultaneously. On the other hand, these are not the energies of the excited and ground states themselves but their difference, $E^e_{\{n\}}-E^g_{\{m\}}$, which defines the frequencies of the Mössbauer resonances. Therefore, there is no need to suppress the contribution of the dipole-dipole interaction to the energies of the excited and ground states; rather, we have to make these contributions equal to each other in order for the frequencies of the Mössbauer transitions to remain unaffected by the dipole-dipole coupling. The following equation expresses this requirement mathematically:

$$\eta_g(3\cos^2\theta^g_{eff}-1) = \kappa\eta_e\left[3\cos^2\left(\frac{\theta^e_{eff}+\theta^g_{eff}}{2}\right) - 1 - \sin^2\left(\frac{\theta^e_{eff}-\theta^g_{eff}}{2}\right)\right], \quad (19)$$

TABLE II. Comparison of the contributions due to the dipole-dipole couplings in the ground, excited, or both ground and excited states to the width of the Mössbauer resonances in the absence of the rf field.

$\Delta\omega_d$ for XL (MHz)	$\Delta\omega_d$ for ZL (MHz)	$\Delta\omega_d$ for ZR (MHz)	$\Delta\omega_d$ for XR (MHz)	$\frac{\eta_g}{2\pi}$ (MHz)	$\frac{\eta_e}{2\pi}$ (MHz)
3.2546	3.3171	3.7089	3.6831	9.024	0
5.9498	3.4867	5.5633	9.3575	0	−5.171
10.9444	7.8394	7.9814	13.8331	9.024	−5.171

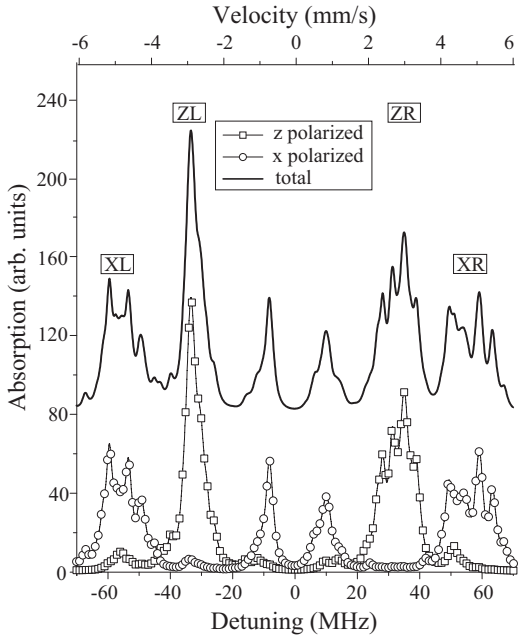

FIG. 8. Mössbauer absorption spectrum broadened due to the dipole-dipole interaction in both ground and excited states in the absence of the rf field. $B_0=30$ T, $\frac{\eta_g}{2\pi}=9.024$ MHz, and $\frac{\eta_e}{2\pi}=-0.573\frac{\eta_g}{2\pi}=-5.171$ MHz. A shift of 80 arbitrary units is introduced to separate the spectrum for unpolarized radiation from its polarized contributions.

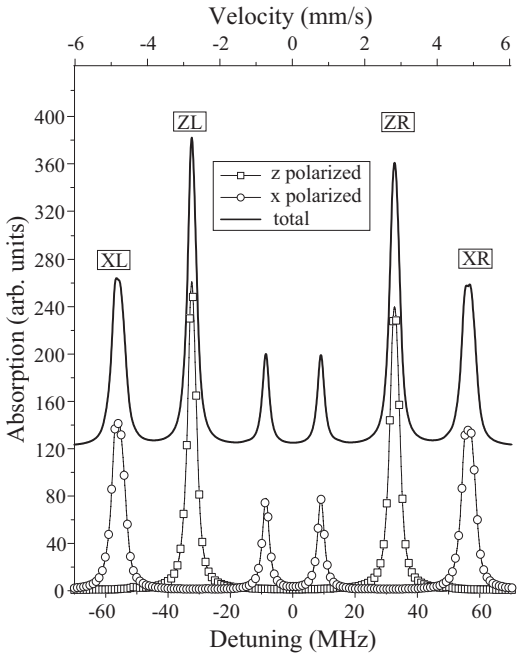

FIG. 9. Mössbauer absorption spectrum calculated in the absence of the rf magnetic field. $B_0=30$ T, $\frac{\eta_g}{2\pi}=2.256$ MHz, and a corresponding $\frac{\eta_e}{2\pi}=-1.2927$ MHz. A shift of 120 arbitrary units is introduced to separate the spectrum for unpolarized radiation from its polarized contributions.

where $\kappa=\pm0.5$, ±1, ±1.5, and ±3. The choice of κ depends on the Floquet states, which contribute to the particular Mössbauer resonance. This condition provides the suppression of the dipole-dipole contribution to a particular Mössbauer resonance by applying only one spinning magnetic field.

We demonstrate it numerically choosing $B_0=30$ T, $\frac{\eta_g}{2\pi}=2.256$ MHz, and $\frac{\eta_e}{2\pi}=\frac{\gamma_e}{\gamma_g}\eta_g=-0.573\eta_g=-1.2927$ MHz.

The initial Mössbauer absorption spectrum (in the absence of the rf field) is shown in Fig. 9. This spectrum has a well-defined Zeeman sextet and a noticeable contribution from the dipole-dipole interaction to the width of Mössbauer resonances. Numerical values of this contribution to the four strongest Mössbauer resonances are given in the first row of Table III.

We calculated the Mössbauer absorption spectra for a broad range of the parameters of the rf field. Figure 10 presents the width of the four strongest Mössbauer resonances as a function of the relative strength r (vertical scale) and the frequency ω_{rf} (horizontal scale) of the rf magnetic field. It clearly follows from Fig. 10 that the regions where maximal suppression of the inhomogeneous broadening is obtained are aligned along thick lines corresponding to the magic-angle condition determined by Eq. (19). Mössbauer resonances with x-polarized radiation are described by the condition with $\kappa=\pm1.5$ (dashed) and $\kappa=\pm3$ (solid), while Mössbauer resonances with z-polarized radiation are described by the condition with $\kappa=\pm0.5$ (dashed) and $\kappa=\pm1$ (solid). When ω_{rf} passes through the resonance for the ground state, κ changes sign since the effective magnetic

TABLE III. Broadening of the four strongest Mössbauer resonances caused by the dipole-dipole interaction for $\frac{\eta_g}{2\pi}=2.256$ MHz and a corresponding $\frac{\eta_e}{2\pi}=-1.2927$ MHz. The last row presents parameters and values corresponding to the case when function defined in Eq. (10) reaches minimum, which means that all four Mössbauer resonances have residual contributions of the same order.

ω_{rf} (MHz)	r	$\Delta\omega_d$ for XL (MHz)	$\Delta\omega_d$ for ZL (MHz)	$\Delta\omega_d$ for ZR (MHz)	$\Delta\omega_d$ for XR (MHz)	Abs min for
0	0	2.648	1.017	1.436	2.894	
33.55	0.4701	0.0809	0.1489	0.0996	0.0920	XL
31.50	0.4000	0.2727	0.0326	0.0722	0.2973	ZL
32.00	0.4310	0.1689	0.0516	0.0591	0.1946	ZR
35.30	0.4504	0.0858	0.1747	0.0934	0.0842	XR
31.90	0.4796	0.1332	0.1568	0.1270	0.1511	Optimal

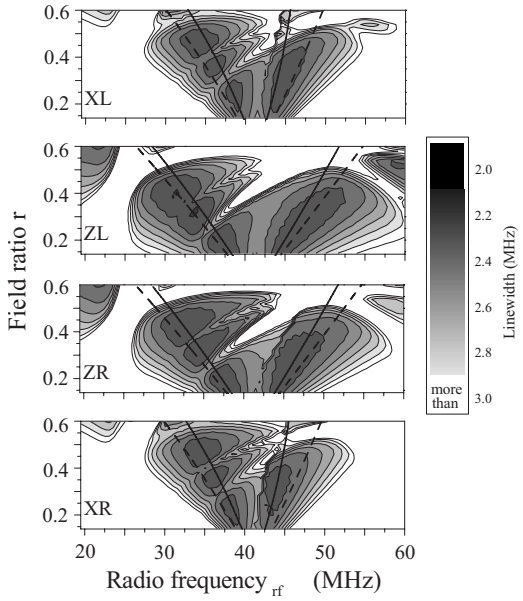

FIG. 10. Dependence of the width of the four strongest Mössbauer resonances on ω_{rf} and r is presented for $B_0=30$ T, $\frac{\eta_g}{2\pi}=2.256$ MHz, and $\frac{\eta_e}{2\pi}=-1.2927$ MHz. The shade coding is used such that the darker shade corresponds to the narrower resonance. To provide better resolution, values greater than 3 MHz are not shown. The regions where maximal suppression of the inhomogeneous broadening is obtained are aligned along thick lines corresponding to the magic-angle condition determined by Eq. (19).

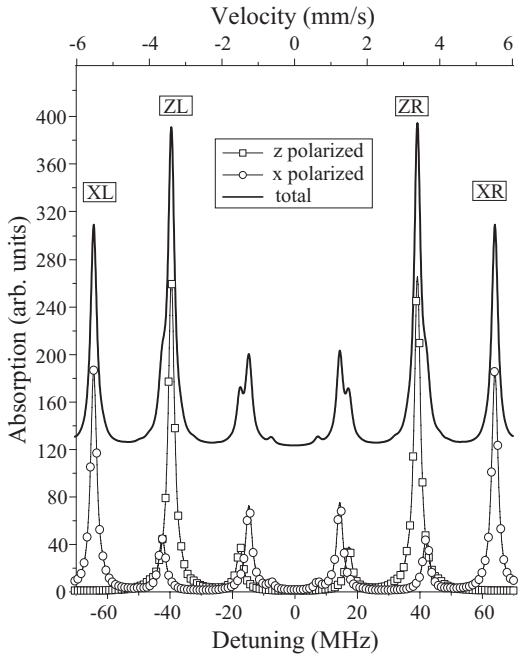

FIG. 11. Mössbauer absorption spectrum calculated in the presence of the spinning magnetic field. It illustrates the Mössbauer line narrowing at the optimal set of the parameters, $r=0.4796$ and $\omega_{rf}=31.90$ MHz. A shift of 120 arbitrary units is introduced to separate the spectrum for unpolarized radiation from its polarized contributions. The residual broadening of the Mössbauer resonances can be found in Table III.

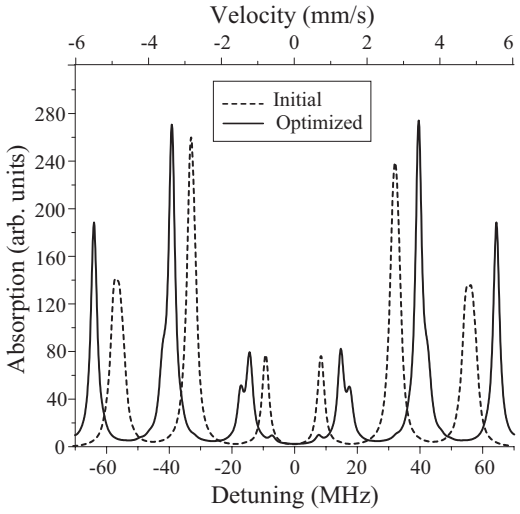

FIG. 12. The comparison of the initial Mössbauer spectrum presented in Fig. 9 with the narrowed spectrum presented in Fig. 11.

field for the ground state changes the direction. Positive κ corresponds to the frequencies below the ground state resonance, and negative κ corresponds to the frequencies above the resonance.

Table III contains the sets of the parameters for which the best line narrowing in the case of individual Mössbauer resonance is achieved. The last row in Table III corresponds to the somewhat balanced case defined by the minimum of the function defined in Eq. (10), when broadening of the four strongest Mössbauer resonances reaches common minimal broadening. The Mössbauer spectrum corresponding to this optimal set of the parameters, $r=0.4796$ and $\omega_{rf}=31.90$ MHz, is presented in Fig. 11. In addition, Fig. 12 compares this optimal configuration with the initial Mössbauer spectrum, presented in Fig. 9. One can easily see that the line narrowing effect takes place.

VIII. CONCLUSION

In this work, we suggested a different technique for suppression of inhomogeneous broadening of Mössbauer resonances. This technique relies on the mutual compensation of the contributions of HF interactions to the ground and excited states rather than total suppression of HF interactions. It is based on the combined action of the continuous wave rf and dc magnetic fields satisfying the specific "magic-angle" condition [Eq. (19)]. This technique is demonstrated numerically in a simple model dealing with a specific HF interaction, namely, the dipole-dipole interaction. It can be generalized for other types of HF interactions, in particular, the quadrupole interaction, exhibiting similar symmetry with respect to rotation.

ACKNOWLEDGMENTS

We gratefully acknowledge the support from the National Science Foundation, the Air Force Office of Science Research, the Office of Naval Research, the Defense Advanced

Research Projects Agency, and the Robert A. Welch Foundation (Grant No. A-1261), and warmly thank Anatoly Andreev, Farit Vagizov, Vladimir Sautenkov, Jos Odeurs, Ercan Alp, Gilbert Hoy, Silviu Olariu, and Andrea Burzo for fruitful discussions. We are grateful to Chris O'Brien for his help in the preparation of this paper.

APPENDIX A: CONCEPT OF EFFECTIVE MAGNETIC FIELD

The Floquet analysis can be used to study behavior of the magnetic moment in the continuous wave rf and dc magnetic fields $\mathbf{B}_{rf}=rB_0[\cos(\omega_{rf}t)\mathbf{x}_0-\sin(\omega_{rf}t)\mathbf{y}_0]$ and $\mathbf{B}_0=B_0\mathbf{z}_0$, respectively. However, an equivalent description in terms of an effective magnetic field is more insightful.

The concept of the effective magnetic field may be introduced by carrying out a transformation to the corotating frame of reference $|\text{old}\rangle=R(-\omega_{rf}t)|\text{new}\rangle$, where $R(\theta)=e^{-i\theta\mathbf{I}\mathbf{z}_0}$ is a rotation operator with a direction of rotation along the z axis. This transformation gives

$$\frac{d}{dt}|\text{new}\rangle=-iH_{new}|\text{new}\rangle, \tag{A1}$$

where $H_{new}=R^{-1}(-\omega_{rf}t)H_{old}R(-\omega_{rf}t)+\omega_{rf}I_z=-\gamma\mathbf{B}_{eff}$. Here, we introduce the effective magnetic field $\mathbf{B}_{eff}=\left(rB_0,0,B_0-\frac{\omega_{rf}}{\gamma}\right)$. The effective magnetic field is time independent and makes an angle with the z axis $\theta_{eff}=\tan^{-1}\left[r\left(1-\frac{\omega_{rf}}{\gamma B_0}\right)^{-1}\right]$. A Zeeman splitting corresponding to this field is $\Delta_{eff}=-\gamma|\mathbf{B}_{eff}|=\Delta\sqrt{\left(1+\frac{\omega_{rf}}{\Delta}\right)^2+r^2}$, where $\Delta=-\gamma|\mathbf{B}_0|$ is a Zeeman splitting in the laboratory frame. Thus, the eigenvalues are Zeeman splittings $E_n=m_{z,n}\Delta_{eff}$ in the effective magnetic field, and the eigenvectors are obtained by rotating the system around the y axis by the angle θ_{eff}:

$$|n\rangle=\sum_{m=-I}^{I}d^I_{m,m_{z,n}}(\theta_{eff})|m\rangle, \tag{A2}$$

where a function $d^I_{m,m_{z,n}}(\theta_{eff})=D^I_{m,m_{z,n}}(0,\theta_{eff},0)$ is an element of the rotation matrix.[41]

An equivalence with the Floquet analysis can be shown by a transformation to the laboratory frame. It gives

$$|n,t\rangle=\sum_{m=-I}^{I}d^I_{m,m_{z,n}}(\theta_{eff})e^{i\omega_{rf}tm}|m\rangle. \tag{A3}$$

This is the Floquet state of the initially time-dependent Hamiltonian corresponding to a quasienergy $E_n=\text{mod}(m_{z,n}\Delta_{eff},\omega_{rf})$.

If the system consists of two noninteracting subsystems, the Floquet states are obtained as a direct product of the Floquet states of individual subsystems $|n,t\rangle=|n_1,t\rangle\otimes|n_2,t\rangle$ with quasienergy $E_n=E_{n_1}+E_{n_2}$.

APPENDIX B: PRESCRIPTION FOR THE FLOQUET ANALYSIS

According to the Floquet theorem in the case of periodic Hamiltonian $H_0(t)$, there is a set of time-dependent Floquet states $|n,t\rangle$ and corresponding quasienergies ϵ_n which satisfy the following conditions: (i) each state is periodic in time $|n,t\rangle=|n,t+T\rangle$, where we have denoted the period by T, and (ii) the quasienergies and the Floquet states satisfy the Schrödinger equation

$$i\frac{\partial}{\partial t}(e^{-i\epsilon_n t}|n,t\rangle)=H_0(t)(e^{-i\epsilon_n t}|n,t\rangle). \tag{B1}$$

In order to avoid inherent ambiguity in a definition of the Floquet states, we always assume that the corresponding quasienergies are chosen in the interval $\epsilon_n\in[0,\omega_{rf}=\frac{2\pi}{T})$. Furthermore, at any fixed time, the Floquet states may be chosen to form an orthonormal basis. This property allows us to write a time evolution operator in terms of the Floquet states as

$$U(t,0)=\sum_n e^{-i\epsilon_n t}|n,t\rangle\langle n,0|, \tag{B2}$$

which obeys the equation $\dot{U}(t,0)=-iH_0(t)U(t,0)$ with an initial condition $U(0,0)=\hat{1}$. The first step is to diagonalize $U(T,0)$ because $U(T,0)=\Sigma_n e^{-i\epsilon_n T}|n,T\rangle\langle n,0|$ is diagonal in the basis of the Floquet states with eigenvalues $\lambda_n=e^{-i\epsilon_n T}$. It is true due to the periodicity condition $|n,T\rangle=|n,0\rangle$. The final step is to propagate the obtained states over the period $|n,t\rangle=e^{i\epsilon_n t}U(t,0)|n,0\rangle$, where we used $\epsilon_n=-\frac{1}{T}\arg(\lambda_n)$ shifted by ω_{rf} to fit the interval $\epsilon_n\in[0,\omega_{rf})$.

*petr@tamu.edu

[1] N. N. Greenwood and T. C. Gibb, *Mössbauer Spectroscopy* (Chapman and Hall, London, 1971).
[2] R. L. Cohen, *Applications of Mössbauer Spectroscopy* (Academic, New York, 1976).
[3] P. Gutlich, R. Link, and A. Trautwein, *Mössbauer Spectroscopy and Transition Metal Chemistry* (Springer-Verlag, Berlin, 1978).
[4] G. R. Hoy, *Encyclopedia of Physical Science and Technology* (Academic, New York, 1992), Vol. 10.
[5] G. J. Long and F. Grandjean, *Mössbauer Spectroscopy Applied to Magnetism and Materials Science* (Plenum, New York, 1993).
[6] J. Hesse and J. B. Muller, Solid State Commun. **22**, 637 (1977).
[7] D. G. Rancourt and J. Y. Ping, Hyperfine Interact. **69**, 497 (1991).
[8] L. A. Rivlin, Gamma-ray laser (1961), USSR patent disclosure.
[9] A. Andreev, Y. A. Il'inskii, and R. V. Khokhlov, Sov. Phys. JETP **40**, 819 (1975).
[10] G. C. Baldwin and J. C. Solem, Rev. Mod. Phys. **69**, 1085 (1997).
[11] U. Haeberlen, *High Resolution NMR in Solids: Selective Averaging* (Academic, New York, 1976).
[12] E. R. Andrew, A. Bradbury, and R. G. Eades, Nature (London) **182**, 1659 (1958).

[13] E. R. Andrew, A. Bradbury, and R. G. Eades, Nature (London) **183**, 1801 (1959).
[14] E. Hahn, Phys. Rev. **80**, 580 (1950).
[15] H. Carr and E. Purcell, Phys. Rev. **94**, 630 (1954).
[16] W. I. Goldburg and M. Lee, Phys. Rev. Lett. **11**, 255 (1963).
[17] M. N. Hack and M. Hamermesh, Nuovo Cimento **19**, 546 (1961).
[18] A. V. Mitin, Sov. Phys. JETP **25**, 1062 (1967).
[19] A. V. Mitin, Opt. Spektrosk. **53**, 288 (1982).
[20] M. Salkola and S. Stenholm, Phys. Rev. A **41**, 3838 (1990).
[21] A. V. Mitin, Izv. Akad. Nauk SSSR, Ser. Fiz. **56**, 186 (1992).
[22] Y. Rostovtsev and O. Kocharovskaya, Hyperfine Interact. **135**, 233 (2001).
[23] L. Pfeiffer, J. Appl. Phys. **42**, 1725 (1971).
[24] M. Kopcewicz, H. G. Wagner, and U. Gonser, Solid State Commun. **48**, 531 (1983).
[25] A. Y. Dzyublik, V. Y. Spivak, R. A. Manapov, and F. G. Vagizov, JETP Lett. **67**, 61 (1998).
[26] F. G. Vagizov, Hyperfine Interact. **61**, 1359 (1990).
[27] F. G. Vagizov, Hyperfine Interact. **61**, 1363 (1990).
[28] I. Tittonen, M. Lippmaa, E. Ikonen, J. Linden, and T. Katila, Phys. Rev. Lett. **69**, 2815 (1992).
[29] M. Lippmaa, I. Tittonen, K. Ullakko, and T. Katila, Hyperfine Interact. **71**, 1345 (1992).
[30] M. Lippmaa, I. Tittonen, J. Linden, and T. Katila, Nucl. Instrum. Methods Phys. Res. B **76**, 146 (1993).
[31] M. Lippmaa, I. Tittonen, J. Linden, and T. Katila, Hyperfine Interact. **92**, 1123 (1994).
[32] M. Lippmaa, I. Tittonen, J. Linden, and T. Katila, Phys. Rev. B **52**, 10268 (1995).
[33] Y. A. Il'inskii and R. V. Khokhlov, Sov. Phys. JETP **38**, 809 (1974).
[34] P. Anisimov, Y. Rostovtsev, and O. Kocharovskaya, J. Mod. Opt. **51**, 2615 (2004).
[35] P. Anisimov, Y. Rostovtsev, and O. Kocharovskaya, J. Mod. Opt. **52**, 2401 (2005).
[36] N. N. Greenwood and T. C. Gibb, *Mössbauer Spectroscopy* (Chapman and Hall, London, 1971), pp. 54–55.
[37] P. Meystre and M. Sargent, *Elements of Quantum Optics* (Springer, New York, 1999).
[38] E. U. Condon and G. H. Shortley, *The Theory of Atomic Spectra* (Cambridge University Press, Cambridge, England, 1935).
[39] I. Tittonen, M. Lippmaa, and J. Javanainen, Phys. Rev. A **53**, 1112 (1996).
[40] C. P. Slichter, *Principles of Magnetic Resonance*, 3rd ed. (Springer-Verlag, Berlin, 1990).
[41] R. N. Zare, *Angular Momentum: Understanding Spatial Aspects in Chemistry and Physics* (Wiley, New York, 1988), p. 89.